

See discussions, stats, and author profiles for this publication at: <https://www.researchgate.net/publication/267910517>

# Reaction Mechanisms for the Formation of Mono- And Dipropylene Glycol from the Propylene Oxide Hydrolysis over ZSM-5 Zeolite

ARTICLE *in* THE JOURNAL OF PHYSICAL CHEMISTRY C · AUGUST 2014

Impact Factor: 4.77 · DOI: 10.1021/jp504432a

---

CITATION

1

READS

78

---

## 5 AUTHORS, INCLUDING:



Pedro Hernandez

Repsol

5 PUBLICATIONS 1 CITATION

[SEE PROFILE](#)



Marcel Swart

Catalan Institution for Research and Advance...

154 PUBLICATIONS 3,434 CITATIONS

[SEE PROFILE](#)



Miquel Solà

Universitat de Girona

398 PUBLICATIONS 8,677 CITATIONS

[SEE PROFILE](#)

# Reaction Mechanisms for the Formation of Mono- And Dipropylene Glycol from the Propylene Oxide Hydrolysis over ZSM-5 Zeolite

Yevhen Horbatenko,<sup>†</sup> Juan Pedro Pérez,<sup>‡</sup> Pedro Hernández,<sup>‡</sup> Marcel Swart,<sup>\*,†,§</sup> and Miquel Solà<sup>\*,†</sup>

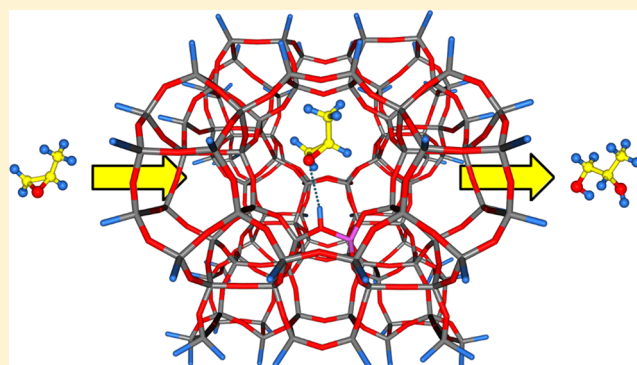
<sup>†</sup>Institut de Química Computacional i Catàlisi, Departament de Química, Campus de Montilivi, Universitat de Girona, 17071 Girona, Catalonia, Spain

<sup>‡</sup>Centro de Tecnología de Repsol, 28935 Móstoles, Madrid, Spain

<sup>§</sup>Institució Catalana de Recerca i Estudis Avançats (ICREA), Pg. Lluís Companys 23, 08010 Barcelona, Spain

## Supporting Information

**ABSTRACT:** Stepwise and concerted mechanisms for the formation of mono- and dipropylene glycol over ZSM-5 zeolite were investigated. For the calculations, a T128 cluster model of zeolite was used with a QM/QM scheme to investigate the reaction mechanism. The active inner part of zeolite was represented by a T8 model and was treated at the DFT (BP86) level, including D3 Grimme dispersion, and the outer part of the zeolite was treated at the DFTB level. The solvent effects were taken into account by including explicitly water molecules in the cavity of the zeolite. The Gibbs energies were calculated for both mechanisms at 70 °C. In the case of the stepwise mechanism for the monopropylene glycol formation, the rate-limiting step is the opening of the epoxide ring. The activation energy for this process is 35.5 kcal mol<sup>-1</sup>, while in the case of the concerted mechanism the rate-limiting step is the simultaneous ring opening of the epoxide and the attack by a water molecule. This process has an activation energy of 27.4 kcal mol<sup>-1</sup>. In the case of the stepwise mechanism of the dipropylene glycol formation, the activation energy for the rate-limiting step is the same as for the monopropylene glycol formation, and in the case of the concerted mechanism, the activation energy for the rate-limiting step is 30.8 kcal mol<sup>-1</sup>. In both cases (mono- and dipropylene glycol formation), the concerted mechanism should be dominant over the stepwise one. The barrier for monopropylene glycol formation is lower than that for dipropylene glycol formation. Consequently, our results show that the formation of the monopropylene glycol is faster, although the formation of dipropylene glycol as a byproduct cannot be avoided using this zeolite.



## INTRODUCTION

Nowadays zeolites are widely used industrial catalysts<sup>1</sup> in a large variety of applications such as skeletal reorganization,<sup>2–4</sup> hydrolysis,<sup>5–8</sup> double bond migration,<sup>9,10</sup> aldol condensation,<sup>11–14</sup> and methylation,<sup>15–18</sup> among others. The last two are of importance since they lead to the formation of new C–C bonds. The advantages of zeolites from an industrial point of view are their high thermal stability, acidity, and shape selectivity. Due to these factors, zeolites not only are essential catalysts in the petroleum industry but also are used in fine chemical synthesis.<sup>1,19</sup>

In industry, the epoxides are obtained from alkenes and hydrogen peroxide using zeolites.<sup>20–23</sup> One of the most important industrial chemical intermediate products is propylene oxide that can be obtained by oxidation of propene by hydrogen peroxide over titanium silica catalyst (Ti/SiO<sub>2</sub>).<sup>5,24</sup> Hydrolysis of this epoxide leads to 1,2-propanediol (monopropylene glycol or MPG), one of the most important chemicals due to its use in a large variety of branches [i.e., unsaturated polyester resins (thermoset plastics, polyurethanes), antifreeze, deicing, heat

transfer fluids, pharmaceuticals (solvent), cosmetics, food, humectants, etc.<sup>25–27</sup>] There are studies dedicated to the mechanism of hydrolysis of epoxides in various media<sup>28–33</sup> as well as over ZSM-5 zeolite.<sup>7,34,35</sup> However, to the best of our knowledge, there are no mechanistic studies of propylene oxide hydrolysis over the ZSM-5 zeolite. To understand the mechanism, we studied theoretically the hydrolysis of propylene oxide over ZSM-5 zeolite to yield MPG. Knowledge of this mechanism is important, since it can help experimentalists to optimize the reaction conditions to increase the yield of desired MPG and to diminish it for undesired dipropylene glycol (DPG) that is obtained as a byproduct of this hydrolysis reaction.

## COMPUTATIONAL METHODS

**Zeolite Models.** Two different models of zeolites were used to perform calculations. The first model is simplified and

**Received:** May 6, 2014

**Revised:** August 27, 2014

**Published:** August 29, 2014

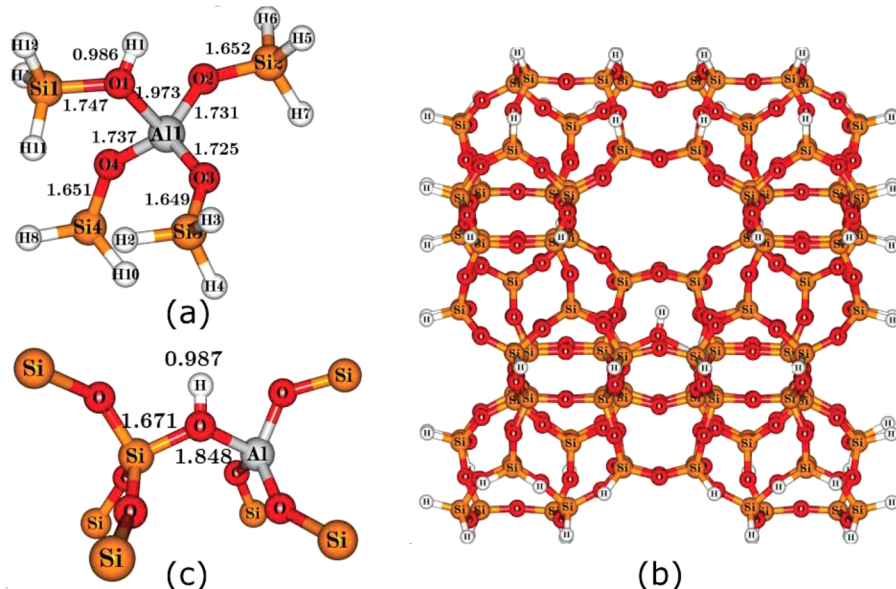


**Figure 1.** Various models that were used to simulate the ZSM-5 zeolite: (a) T5 simplified model of the zeolite; (b) T128 cluster model of the zeolite; and (c) T8 model that represents the inner layer of the T128 cluster.

represents the active site of the zeolite. It includes 5 tetrahedral atoms (T5) (i.e., four silicons and one aluminum [ $\text{Al}(\text{OSiH}_3)_4$ ]) (see Figure 1a). This allowed a detailed analysis of different reaction pathways and different conformations of intermediates, transition states, and products. The results, obtained using this model, were very useful to study the hydrolysis using a larger model of the zeolite. It is worth noting that in the work of ref 36, the authors considered the small model T5 as well as a larger T63 model to investigate proton transfer reactions inside the cavity of ZSM-5 toward various bases. In accordance with their results, optimized geometries of the products obtained using both these models are rather similar and T5 clusters could be used to obtain reasonable estimations for the adsorption energies.

The second model is represented by 128 tetrahedral atoms (T128) (i.e., 127 silicons and 1 aluminum) (see Figure 1b). This cluster model includes the intersection of zigzag and straight channels. The model was taken from the crystallographic structure<sup>37–39</sup> of a ZSM-5 zeolite. The cut Si–O bonds were terminated with H atoms with a Si–H distance of 1.47 Å.

The calculations were done using the QM/QM methodology, and within this methodology the T128 cluster was divided into two layers. The inner layer was represented by a T8 model (see Figure 1c) that includes seven silicon atoms and one aluminum atom and was somewhat larger than the T5 model used in the first part of our study. This T8 model belongs to the 10-membered ring that is formed by the intersection of straight and zigzag channels and includes the active site of the zeolite where the reaction occurs. The inner layer was treated at a high level of theory, and the rest of the structure (outer layer) was treated at a lower level of theory using the approximate density functional tight-binding (DFTB) approach.<sup>40–44</sup>

**DFT(B) Calculations.** All geometry optimizations and transition state searches were performed using the ADF<sup>45–47</sup> package. The QUILD<sup>48</sup> program was used as a wrapper around ADF/DFT(B), since it has an improved geometry optimization technique (i.e., with adapted delocalized coordinates).<sup>49</sup> QUILD was used to construct the input for ADF/DFT(B), to run ADF/

DFT(B), and to collect the data. ADF and DFTB were used only to calculate gradients and energies.

With ADF for the T5 simple model and for the T8 model of the inner layer of T128, the BP86<sup>50,51</sup> functional was used along with the D3 method<sup>52</sup> of Grimme to take into account dispersion effects. The DZP basis set<sup>53</sup> was used for all atoms: carbon, hydrogen, oxygen, silicon, and aluminum; core electrons were treated using the frozen core approximation.<sup>47</sup> To include the solvent effects (aqueous solution) in the case of T5 model, the COSMO<sup>54–57</sup> model was used. For the low-level QM description in the case of T128, the DFTB semiempirical approach was used using the Dresden parameters that are available within the ADF program package.<sup>41–44,58</sup>

In the T5 model, no geometrical constraints were imposed. In the T128 model, only the T8 fragment was allowed to relax, while the rest of the geometry was maintained frozen to prevent the zeolite from any distortion. For the cluster model T128, nine explicit water molecules were considered (i.e., eight in the outer layer that were described with DFTB, and one in the inner layer). The water molecules were included in such a way that they surrounded propylene oxide together with the reaction center of the zeolite. The straight channel and the zigzag channel were filled with 5 and 3 water molecules, respectively. The water molecule from the inner layer participated in the reaction and, thus, was described at the BP86-D3/DZP level. The water molecules both from the outer and inner layers were allowed to relax during geometry optimizations.

In the case of the T5 model, the vibrational frequencies were calculated to verify the nature of all stationary points (i.e., minima and transition states at the same level of theory as optimization were done). In the case of the T128 model, the vibrational frequencies were not obtained since it was not possible to calculate them with the outer layer frozen. Finally, the Gibbs free energies at 70 °C for the T128 cluster model were approximated using at each step the thermal corrections and entropies calculated for the T5 model. These terms were not calculated for the T128 cluster model due to technical issues. We believe that this is a reasonable approximation. The Gibbs free energies were calculated according to the equation:

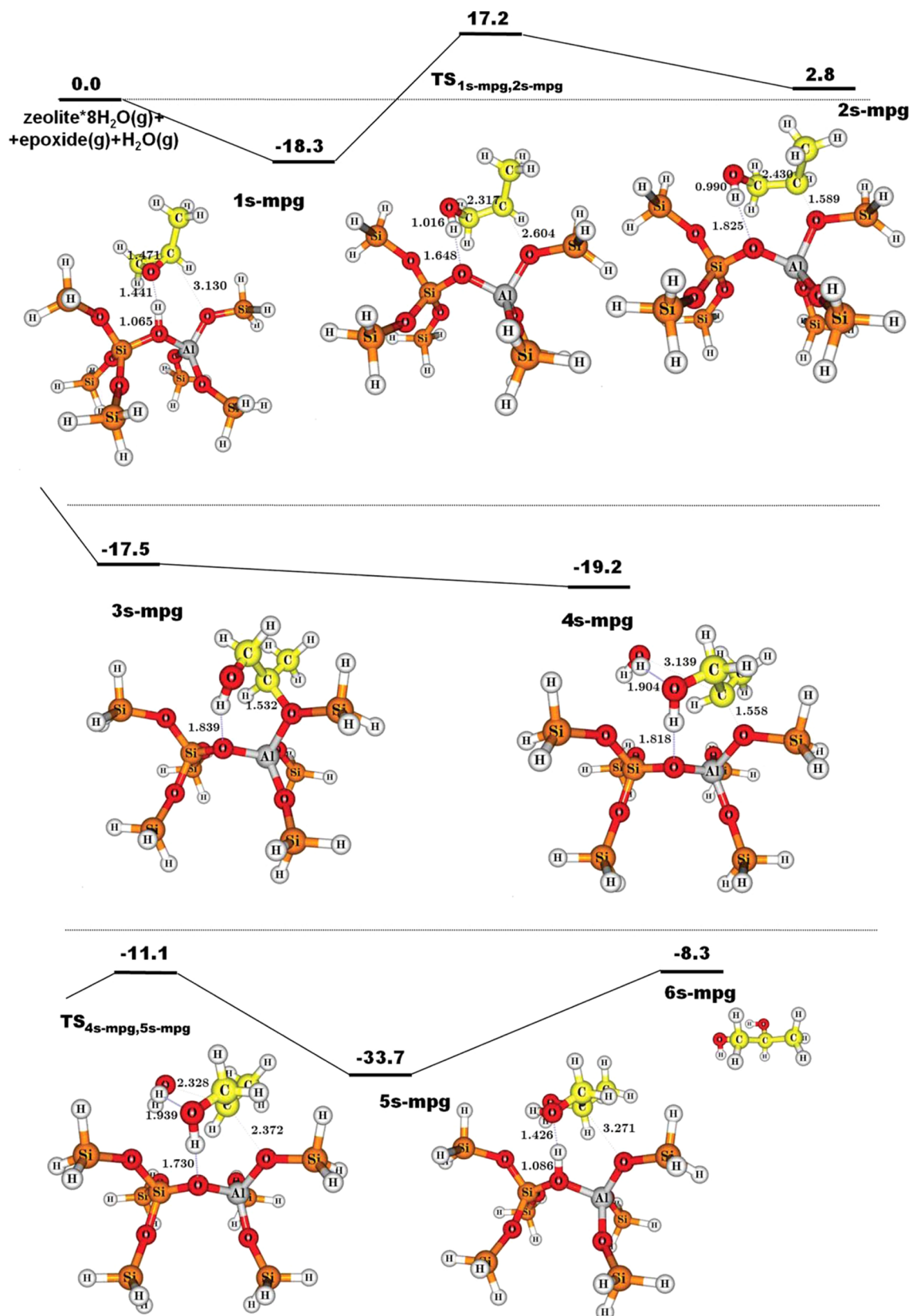


**Figure 2.** Stepwise mechanism for monopropylene glycol formation. For the sake of clarity, only the propylene epoxide, active water molecule, and T8 part of T128 model of the zeolite are shown. Relative energies in kcal mol<sup>-1</sup> are Gibbs energies.

$$G = [(E + ZPE + C_v T) + nRT] - TS \quad (1)$$

where  $E$  is the electronic internal energy, ZPE is the zero-point energy,  $C_v$  is the heat capacity at constant volume,  $n$  is the number of moles,  $R$  is the gas constant,  $T$  is the temperature, and

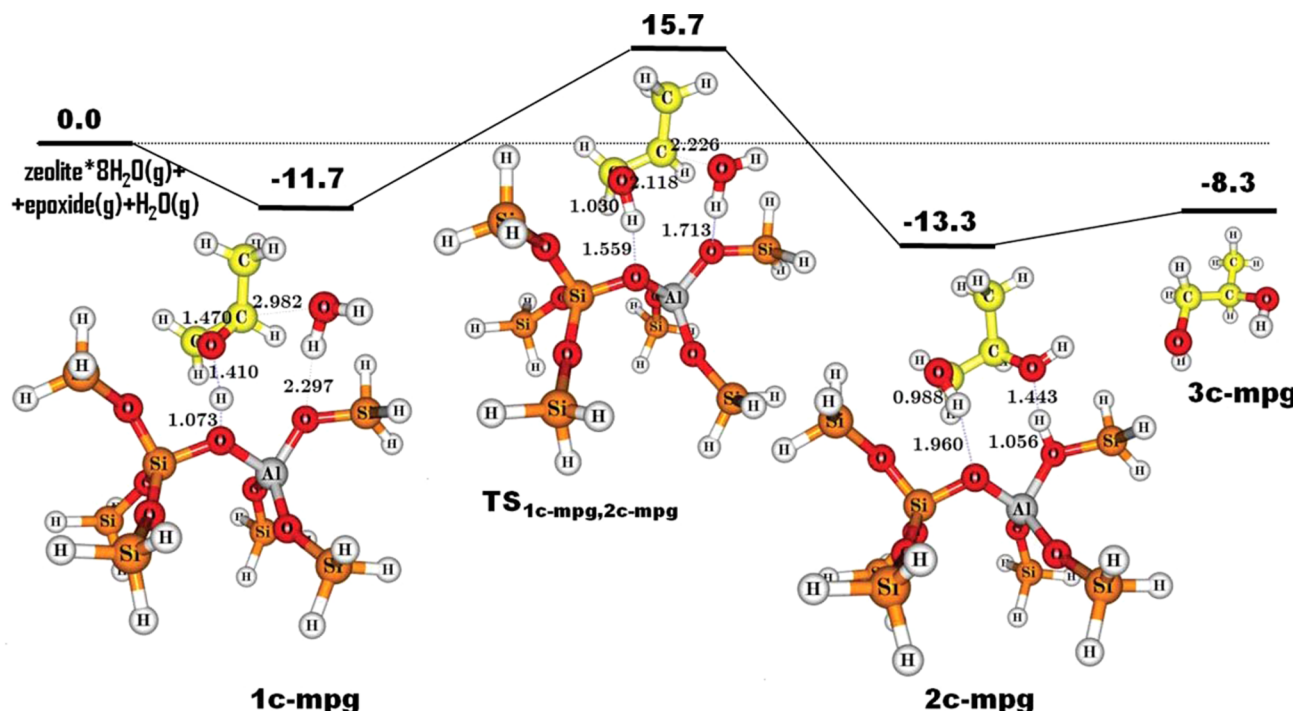


**Figure 3.** Concerted mechanism for monopropylene glycol formation. For the sake of clarity, only the propylene epoxide, active water molecule, and T8 part of T128 model of the zeolite are shown. Relative energies in  $\text{kcal mol}^{-1}$  are Gibbs energies.

$S$  is the entropy.  $E + \text{ZPE} + C_v T$  constitute the internal energy,  $U$ , that along with the  $nRT$  term gives the enthalpy,  $H$ . Catalytic hydration of propylene oxide over ZSM-5 occurs even at room temperature. Some of us have performed experimentally the hydration of propylene oxide in ZSM-5 at  $70^\circ\text{C}$ . At this temperature, one gets relatively large reaction rates with a low byproduct formation (basically due to dehydration of the 1,2-propanediol). For this reason, Gibbs energy calculations of the reaction were performed at  $70^\circ\text{C}$ .

## RESULTS AND DISCUSSION

When the molecule of propylene oxide is diffused into a cavity of zeolite, an adduct between zeolite and epoxide is formed due to hydrogen bonding. The adduct formation occurs on the zeolite Brønsted acid site. Further transformations of this adduct can proceed via stepwise or concerted mechanisms. Both of them will be considered here.

**T5 Simple Model.** The mechanisms for MPG and undesirable DPG (byproduct) formation using the simple T5 model in aqueous solution were calculated (full detailed information on the results for both stepwise and concerted mechanisms can be found in the Supporting Information). The results of our calculations showed that the concerted mechanism for MPG formation is favored by approximately  $7 \text{ kcal mol}^{-1}$  compared to the stepwise one. A similar situation was found for the formation of DPG (i.e., the concerted mechanism is favored by approximately  $10 \text{ kcal mol}^{-1}$ ). Both thermodynamics and kinetics showed that the formation of DPG over T5 is somewhat more favorable than the formation of MPG. Thus, one could expect the formation of a mixture of products (see the Supporting Information).

**T128 Cluster Model. Stepwise Mechanism for Monopropylene Glycol Formation.** The stepwise mechanism (an epoxide ring opening and then attack with a water molecule) is represented in Figure 2. In this mechanism, we start with a ZSM-

5 zeolite of mordenite framework inverted (MFI) structure, propylene oxide, a water molecule as reactive species, and eight molecules of water which are “spectators”. In the first step, the propylene oxide is adsorbed over the acidic center of the zeolite. The interaction of the propylene oxide with the zeolite and with the rest of the eight water molecules produces an intermediate **1s-mpg**, which is stabilized by about  $18 \text{ kcal mol}^{-1}$  relative to the zeolite\* $8\text{H}_2\text{O}$  and epoxide reactants (see Figure 2). In this intermediate, the hydrogen bond interaction between the O atom of the epoxide and the acidic H of the zeolite leads to the elongation of the OH bond from  $0.987$  to  $1.065 \text{ \AA}$ . Then, the simultaneous proton transfer from the zeolite to the O atom of the epoxide and the ring opening occur through the transition state **TS<sub>1s-mpg,2s-mpg</sub>**. During this process, the OH of the zeolite elongates from  $1.065$  to  $1.648 \text{ \AA}$ . The rupture of the  $\text{C}_{\beta(\text{secondary})}-\text{O}_{\text{epoxide}}$  bond leads to its elongation from  $1.471$  to  $2.317 \text{ \AA}$ , and the bond  $\text{C}_{\beta(\text{secondary})}-\text{O}_{\text{zeolite}}$  shortens from  $3.130$  to  $2.604 \text{ \AA}$ . The transition state has a barrier of  $35.5 \text{ kcal mol}^{-1}$  relative to the intermediate **1s-mpg**. This transition state was confirmed using the T5 model (see the Supporting Information). It has only one imaginary frequency ( $297\text{i cm}^{-1}$ ) that is related to the proton transfer from the zeolite to the epoxide and to the epoxide ring opening. This would be the limiting step of the reaction. It is worth mentioning that this barrier decreases substantially when more water molecules are included. Specifically, in the T128 model with 18 water molecules, the barrier is reduced to  $24.3 \text{ kcal mol}^{-1}$ . Thus, the model with more water molecules is more consistent with experimental results, showing that this reaction proceeds smoothly at  $70^\circ\text{C}$ . A total of about 18 water molecules is the maximum number of molecules that can be introduced into the spherical cavity of the zeolite. However, the computational cost of this model is too high due to the large number of configurations of similar energy that can adopt the water molecules, and we used it only to study this limiting step of the whole process.

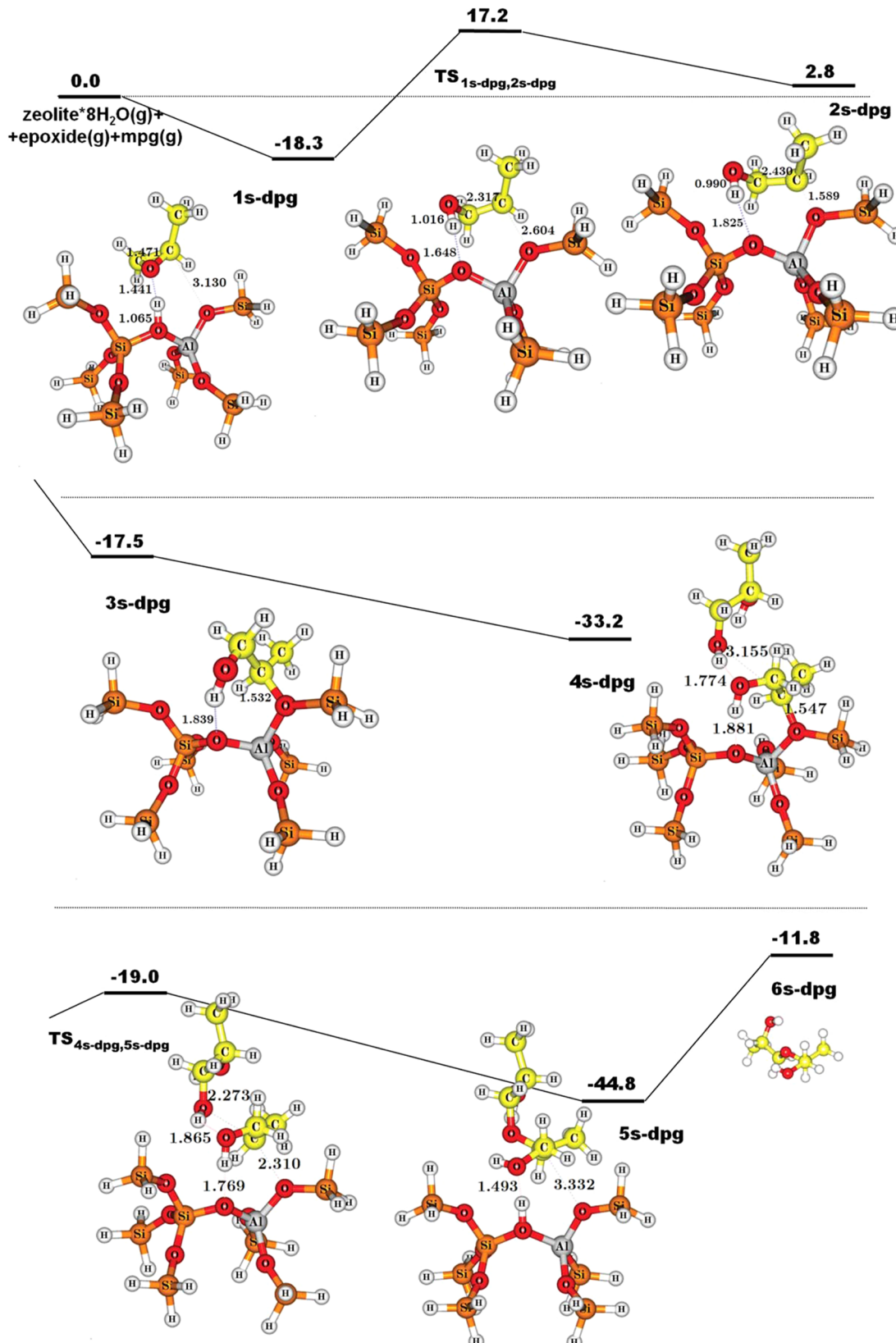


**Figure 4.** Stepwise mechanism for dipropylene glycol formation. For the sake of clarity, only the propylene epoxide, monopropylene glycol, and T128 part of the T128 model of the zeolite are shown. Relative energies in  $\text{kcal mol}^{-1}$  are Gibbs energies.

The result of the previous step is the formation of the alcohol **2s-mpg**. During this formation step, the  $C_{\beta(\text{secondary})}-\text{O}_{\text{zeolite}}$  distance changes from 2.604 in the transition state to 1.589 Å

in **2s-mpg**. Then, **2s-mpg** undergoes a conformational change leading to **3s-mpg**. The  $C_{\beta(\text{secondary})}-\text{O}_{\text{zeolite}}$  distance shortens by 0.05 Å in this process to 1.532 Å in **3s-mpg**. The stabilization

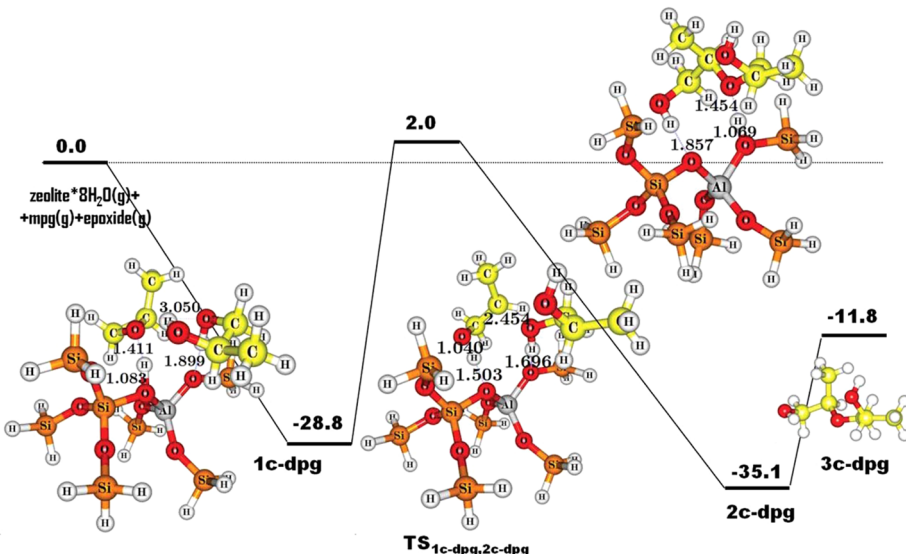


**Figure 5.** Concerted mechanism for dipropylene glycol formation. For the sake of clarity, only the propylene epoxide, monopropylene glycol, and T8 part of the T128 model of the zeolite are shown. Relative energies in kcal mol<sup>-1</sup> are Gibbs energies.

energy in this process is 20.3 kcal mol<sup>-1</sup>. This stabilization can be related to the vanishing of a steric hindrance, due to the presence of the methyl group, after rotation. The corresponding transition state for the conformational change was not studied because it is expected that the barrier for such a conformational change is low and does not have a large influence on the entire process. The interaction of **3s-mpg** with the water molecule, which is treated at the high level in our model, gives rise to the formation of an epoxide–water coadsorption complex **4s-mpg**, which leads to additional stabilization of 1.7 kcal mol<sup>-1</sup> and to the small lengthening of the  $C_{\beta(\text{secondary})}$ –O<sub>zeolite</sub> bond from 1.532 to 1.558 Å. Afterward, the S<sub>N</sub>2 reaction occurs through the **TS<sub>4s-mpg,5s-mpg</sub>** transition state, where the oxygen of water attacks the secondary carbon atom of the alcohol. A shortening of the O<sub>water</sub>–C<sub>β(secondary)</sub> (from 3.139 to 2.328 Å) distance occurs at the same time with the lengthening of the  $C_{\beta(\text{secondary})}$ –O<sub>zeolite</sub> (from 1.558 to 2.372 Å) distance. The transition state **TS<sub>4s-mpg,5s-mpg</sub>** has a barrier of 8.1 kcal mol<sup>-1</sup> with respect to the intermediate **4s-mpg**. This transition state was confirmed again using the T5 model (see the Supporting Information). It has only one imaginary frequency (84i cm<sup>-1</sup>) that is related to the breaking of the  $C_{\beta(\text{secondary})}$ –O<sub>zeolite</sub> bond and to the formation of the O<sub>water</sub>–C<sub>β(secondary)</sub> bond simultaneously. Upon the formation of the O<sub>water</sub>–C<sub>β(secondary)</sub> bond, the hydrogen atom starts to move toward the O of the zeolite. The S<sub>N</sub>2 reaction leads to adsorbed 1,2-propanediol **5s-mpg**. Final desorption of the products to give desorbed 1,2-propanediol **6s-mpg** and to recover the initial catalyst has an energy cost of 25.4 kcal mol<sup>-1</sup>. Therefore, the total reaction is exothermic by 8.3 kcal mol<sup>-1</sup>.

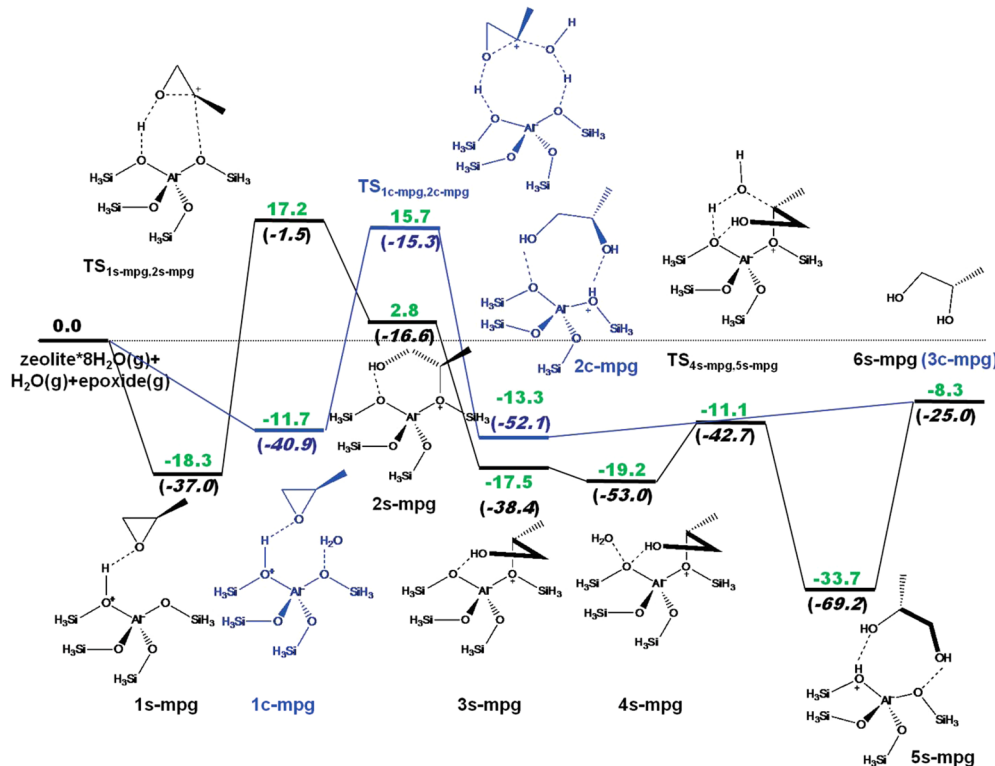
**Concerted Mechanism for Monopropylene Glycol Formation.** The concerted mechanism (simultaneous epoxide ring opening and the attack with a water molecule) obtained in the presence of 9 water molecules is represented in Figure 3. Similar to that above, in this mechanism we start with the zeolite ZSM-5 that is interacting with 8 “spectator” water molecules, propylene oxide, and a water molecule that participates in the reaction. The initial step is the adsorption of the epoxide on the acid site of the zeolite and the coadsorption of a water molecule next to the epoxide. The interaction between the adsorbed propylene oxide and a water molecule over the zeolite and with the rest of the

water molecules leads to a stabilization of −11.7 kcal mol<sup>-1</sup> and generates intermediate **1c-mpg** (see Figure 3). After the formation of this intermediate, the elongation of the OH bond in zeolite from 0.987 to 1.073 Å occurs due to the hydrogen bond interaction between the O atom of the epoxide and the acidic H of the zeolite. In this intermediate, the water molecule is weakly coadsorbed. The distance between the H of the water molecule and the O atom of the zeolite is 2.297 Å and that between the C<sub>β(secondary)</sub> of the epoxide and the O atom of the water is 2.982 Å. Then, the ring opening occurs simultaneously with the attack of the water molecule through the transition state **TS<sub>1c-mpg,2c-mpg</sub>** that involves a simultaneous double proton transfer. During the ring opening, the distances O<sub>zeolite</sub>–H<sub>water</sub> and O<sub>water</sub>–C<sub>β(secondary)</sub> shorten from 2.297 to 1.713 Å and from 2.982 to 2.226 Å, respectively, while C<sub>β(secondary)</sub>–O<sub>epoxide</sub> and O<sub>zeolite</sub>–H<sub>zeolite</sub> bonds lengthen from 1.470 to 2.118 Å and from 1.073 to 1.559 Å, correspondingly. The barrier of this ring opening is of 27.4 kcal mol<sup>-1</sup> relative to the intermediate **1c-mpg**. This transition state has only one imaginary frequency (286i cm<sup>-1</sup>) that was obtained using the T5 model (see the Supporting Information). The frequency corresponds to the proton transfer from zeolite to epoxide and to the epoxide ring opening along with attack of C<sub>β(secondary)</sub> of the epoxide by a water molecule. This leads to the formation of the adsorbed monopropylene glycol **2c-mpg** at the zeolite interacting with the 8 “spectator” water molecules. This energy barrier is reduced by 4.9 kcal mol<sup>-1</sup> if 18 water molecules are considered in the reaction medium. Finally, the desorption process of MPG and recovery of the initial zeolite costs 5.0 kcal mol<sup>-1</sup>.

Both mechanisms present the same exothermicity but the barrier of the determining step is somewhat lower for the concerted mechanism (22.5 kcal mol<sup>-1</sup>, best estimate) than that for the stepwise mechanism (24.3 kcal mol<sup>-1</sup>, best estimate). This energetic difference is too small to completely rule out the stepwise mechanism, though our calculations show a preference for the concerted mechanism.

**Stepwise Mechanism for Dipropylene Glycol Formation.** The stepwise mechanism for the DPG formation is shown in Figure 4. The first few steps of the mechanism coincide with those for hydrolysis of the propylene oxide to MPG until the step

**Scheme 1.** Comparison of Stepwise and Concerted Mechanisms in Acid Medium in the Presence of Catalyst for Monopropylene Glycol Formation. The Numbers in Green Are Relative Gibbs Energies at 70 °C and the Numbers in Blue or Black Are Relative Electronic Energies



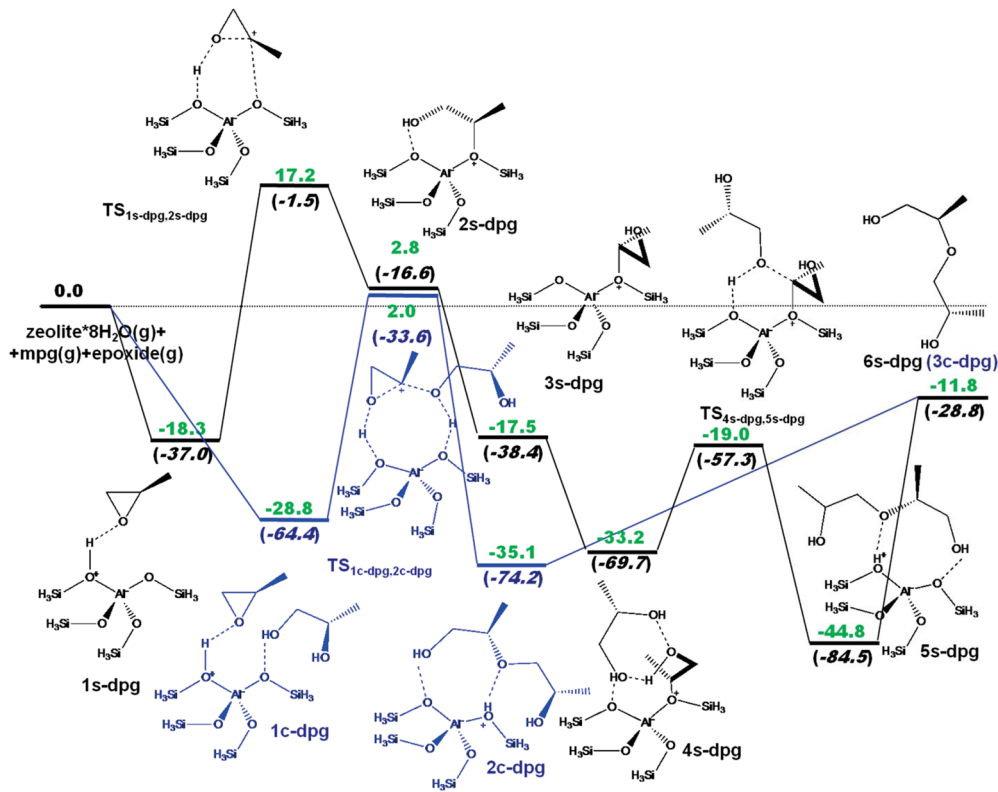
where 1,2-propylene glycol enters the reaction instead of a water molecule (i.e., the formation of the intermediate **4s-dpg** where MPG molecule interacts with the intermediate **3s-dpg**). The stabilization of 15.8 kcal mol<sup>-1</sup> in this case is greater than that from the interaction with a water molecule (1.7 kcal mol<sup>-1</sup>). Upon the formation of **4s-dpg** from **3s-dpg**, the C<sub>β(secondary)</sub>—O<sub>zeolite</sub> distance changes from 1.532 to 1.547 Å. Finally, through the S<sub>N</sub>2 transition state **TS<sub>4s-dpg,5s-dpg</sub>** with a barrier of 14.2 kcal mol<sup>-1</sup>, the formation of the adsorbed dipropylene glycol **5s-dpg** occurs. In this transition state the oxygen of MPG attacks the secondary carbon atom of alcohol. The O<sub>MPG</sub>—C<sub>β(secondary)</sub> distance shortens from 3.155 to 2.273 Å at the same time the C<sub>β(secondary)</sub>—O<sub>zeolite</sub> distance gets longer by 0.763 Å (from 1.547 to 2.310 Å). This transition state has only one imaginary frequency (196*i* cm<sup>-1</sup>) that corresponds to the simultaneous breaking of the C<sub>β(secondary)</sub>—O<sub>zeolite</sub> bond and formation of the O<sub>MPG</sub>—C<sub>β(secondary)</sub> bond. The nature of the transition state was confirmed using the TS model (see the Supporting Information). The hydrogen returns to the O of the zeolite when the distance O<sub>MPG</sub>—C<sub>β(secondary)</sub> shortens. Final desorption of DPG from zeolite has a relatively high energy cost of 33.0 kcal mol<sup>-1</sup>. The total reaction is more exothermic than the reaction for MPG formation (11.8 kcal mol<sup>-1</sup>).

**Concerted Mechanism for Dipropylene Glycol Formation.** The concerted mechanism for the dipropylene glycol formation obtained in the presence of nine water molecules is represented in Figure 5. As in the previous case, in this mechanism we start with the ZSM-5 zeolite that is interacting with eight spectator water molecules, propylene oxide, and one molecule of MPG that participates in the reaction. In the first step, due to the adsorption of the epoxide on the acid site of the zeolite and the coadsorption of MPG molecule next to the epoxide, the

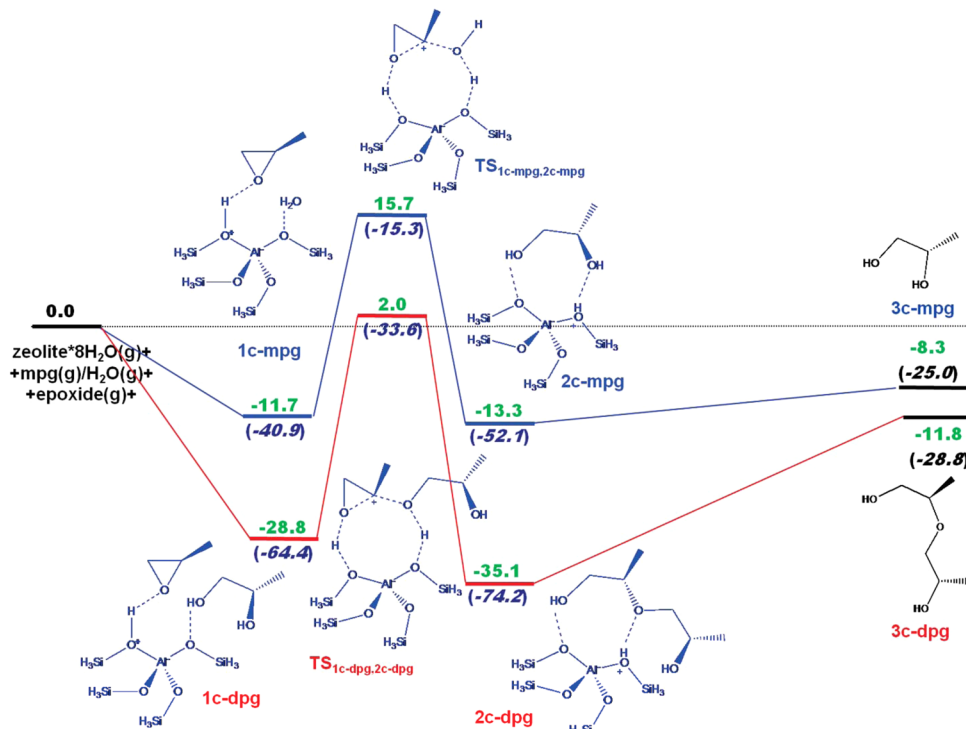
interaction between propylene oxide and MPG and the rest of the water molecules leads to a stabilization of 28.8 kcal mol<sup>-1</sup> and generates the intermediate **1c-dpg** (see Figure 5). When this intermediate is formed, the OH distance in zeolite changes from 0.987 to 1.083 Å. The H<sub>water/MPG</sub>—O<sub>zeolite</sub> distance is longer in the case of the adsorbed water than in the case of the adsorbed monopropylene glycol. This is due to the stronger adsorption of the latter. The simultaneous ring opening and the attack of MPG molecule goes through the transition state **TS<sub>1c-dpg,2c-dpg</sub>**. In this process, the distances O<sub>zeolite</sub>—H<sub>MPG</sub> and O<sub>MPG</sub>—C<sub>β(secondary)</sub> shorten from 1.899 to 1.696 Å and from 3.050 to 2.454 Å, respectively. The OH bond of the zeolite changes from 1.083 to 1.503 Å. The barrier of this transition state is 30.8 kcal mol<sup>-1</sup> relative to the intermediate **1c-dpg**. The nature of the transition state was confirmed using the TS model (see the Supporting Information). It has only one imaginary frequency (266*i*) that corresponds to the proton transfer from the zeolite to the epoxide and to the epoxide ring opening along with attack of C<sub>β(secondary)</sub> of the epoxide by the MPG molecule. Afterward, the adsorbed dipropylene glycol **2c-dpg** forms at the zeolite ZSM-5 interacting with the 8 “spectator” water molecules. The final desorption to give dipropylene glycol **3c-dpg** needs the energy of 23.3 kcal mol<sup>-1</sup>.

**Comparison between Stepwise and Concerted Mechanisms.** This section compares the stepwise and concerted mechanisms for the formation of MPG and DPG. Scheme 1 shows the results for the comparison of the MPG formation. In both cases, the results were obtained in the same conditions. Obviously from a thermodynamic point of view there is no difference between the two reaction mechanisms because they start from the same reactants and come to the same products. The major difference is observed in the first step where the

**Scheme 2.** Comparison of Stepwise and Concerted Mechanisms in Acid Medium in the Presence of Catalyst for Dipropylene Glycol Formation. The Numbers in Green Are Relative Gibbs Energies at 70 °C and the Numbers in Blue or Black Are Relative Electronic Energies



**Scheme 3.** Comparison between Concerted Mechanisms in Acid Medium in the Presence of Catalyst for Mono- and Dipropylene Glycol Formation. Numbers in Green are Relative Gibbs Energies at 70 °C and Numbers in Blue or Black are Relative Electronic Energies



concerted mechanism has a barrier of 27.4 kcal mol<sup>-1</sup> (Gibbs energy) while that for a stepwise mechanism is 35.5 kcal mol<sup>-1</sup>

(Gibbs energy). As we have seen, these barriers are reduced when considering a model with more water molecules. However, there

is still a non-negligible difference in energy barriers that allows the conclusion that the operating mechanism is a concerted reaction mechanism.

Scheme 2 compares the stepwise and concerted mechanisms that lead to the formation of DPG. Again the barrier for the concerted mechanism is lower ( $30.8 \text{ kcal mol}^{-1}$ ) than the barrier for the stepwise process ( $35.5 \text{ kcal mol}^{-1}$ ). The comparison shows that the energy barrier for DPG formation is greater than that for MPG formation.

With regard to the mechanism, it is important to note two things. First, studies by Long and Pritchard<sup>29</sup> concluded that the mechanism was of  $S_N1$  type (stepwise mechanism), but these were performed in the absence of zeolite and hence the mechanism may be different in solution and in the presence of zeolite. Second, in the articles of Lundin<sup>32</sup> et al. and Filho<sup>33</sup> et al., in which the acid catalysis without zeolite was studied, the  $S_N1$  mechanism was discarded and it was concluded that the concerted  $S_N2$  mechanism was more favorable. The article of Filho et al. explains the experimental results obtained by Long and Pritchard without resorting to the  $S_N1$  mechanism. On the other hand, there are reactions related to our study which proceed in zeolites through the concerted mechanism.<sup>8</sup> On the basis of the data we have from the literature and with the results we have obtained, we conclude that the concerted  $S_N2$  mechanism is the mechanism that operates in this hydrolysis.

**Comparison between Concerted Mechanisms for Mono- and Dipropylene Glycol Formation.** Since the concerted mechanism gives lower barriers according to our calculations, in this section we compare the concerted reaction mechanism profiles for the formation of MPG and DPG. The results are shown in Scheme 3. As one can see, the reaction that leads to the DPG formation is more exothermic (by  $3.5 \text{ kcal mol}^{-1}$ ) than that for the MPG formation. However, the barrier associated with the process that results in DPG ( $30.8 \text{ kcal mol}^{-1}$ ) is somewhat larger than the barrier for MPG ( $27.4 \text{ kcal mol}^{-1}$ ). In the presence of a larger number of water molecules, these barriers would be reduced by about  $5 \text{ kcal mol}^{-1}$ . In accordance with these results, the MPG formation is faster than the DPG. However, the latter is thermodynamically more favorable. Consequently, both MPG and DPG are formed during the reaction as confirmed experimentally.

Since DPG occupies a larger volume than MPG, one possible way of increasing the yield of the latter and reducing that of the former is to inhibit, sterically, the formation of DPG. It is known that the diameter of the channels in ZSM-5 is about  $5.1\text{--}5.6 \text{ \AA}$ ,<sup>59,60</sup> and a maximum diameter of a sphere that can diffuse along these channels is about  $4.5 \text{ \AA}$ .<sup>61</sup> Thus, one can use zeolites with a smaller channel size where MPG could be formed and could be diffused easily, but DPG formation and diffusion would be prevented.

## CONCLUSIONS

This work presents a study on the hydrolysis of propylene oxide to mono- or dipropylene glycol over the ZSM-5 zeolite. Two different mechanisms for mono- and dipropylene glycol formation were considered: stepwise and concerted. In the case of the stepwise mechanism for the monopropylene glycol formation, the reaction proceeds via the ring opening of the epoxide. This rate-determining step has a barrier of  $35.5 \text{ kcal mol}^{-1}$  ( $24.3 \text{ kcal mol}^{-1}$ , best estimate). The attack by a water to form the monopropylene glycol goes through a transition state with a barrier of  $8.1 \text{ kcal mol}^{-1}$ . In the case of the concerted mechanism for the monopropylene glycol formation, the ring

opening and the attack by a water molecule occurs at the same time. This step is rate determining with a barrier of  $27.4 \text{ kcal mol}^{-1}$  ( $22.5 \text{ kcal mol}^{-1}$ , best estimate). This difference in energy barriers indicates that the concerted mechanism is likely to be the operating one.

For the stepwise mechanism for the dipropylene glycol formation, the rate-determining step (ring opening) has the same height of the barrier as that for the monopropylene glycol formation ( $35.5 \text{ kcal mol}^{-1}$ ). The subsequent attack by monopropylene glycol molecule to form a dipropylene glycol goes through a transition state that has a barrier of  $14.2 \text{ kcal mol}^{-1}$ . For the concerted mechanism for the dipropylene glycol formation where the ring opening and the attack by monopropylene glycol molecule occurs at the same time, the barrier is  $30.8 \text{ kcal mol}^{-1}$ . In this case, one can conclude that the operating mechanism for the formation of dipropylene glycol is the concerted one as well.

The comparison between two concerted mechanisms reveals that the barrier for the monopropylene glycol formation is lower than that for the dipropylene glycol formation. Thus, the formation of the former is faster. However, the latter is more stable thermodynamically. Finally, the use of zeolite with smaller channels should help to prevent DPG formation as byproduct of the propylene oxide hydrolysis reaction.

## ASSOCIATED CONTENT

### Supporting Information

Discussion on the stepwise and concerted mechanisms of the propylene oxide hydrolysis to the monopropylene glycol and to the dipropylene glycol over T5 simplified model of the zeolite (solvent effects are included). Cartesian coordinates of all optimized minima and transition state geometries for stepwise and concerted mechanisms of the propylene oxide hydrolysis over T5 and T128 zeolite models. Complete ref 45. This material is available free of charge via the Internet at <http://pubs.acs.org>.

## AUTHOR INFORMATION

### Corresponding Authors

\*E-mail: marcel.swart@udg.edu. Tel: (+34) 972 418861.

\*E-mail: miquel.sola@udg.edu. Tel: (+34) 972 418912.

### Notes

The authors declare no competing financial interest.

## ACKNOWLEDGMENTS

The following organizations are thanked for financial support: REPSOL company (project entitled “Application of computational chemistry in catalysis”), the Ministerio de Ciencia e Innovación (MICINN, project numbers CTQ2011-23156/BQU and CTQ2011-25086/BQU), the Generalitat de Catalunya (Grants 2009SGR637, 2009SGR528, 2014SGR931, and Xarxa de Referència en Química Teòrica i Computacional), and the FEDER fund (European Fund for Regional Development) for Grant UNGI08-4E-003. Y.H. thanks the Universitat de Girona for an employment contract. Support for the research of M.S. was received through the ICREA Academia 2009 prize for excellence in research funded by the DIUE of the Generalitat de Catalunya. Excellent service by the Centre de Serveis Científics i Acadèmics de Catalunya (CESCA) is gratefully acknowledged.

## ■ REFERENCES

- (1) Sen, S. E.; Smith, S. M.; Sullivan, K. A. Organic Transformations Using Zeolites and Zeotypes Materials. *Tetrahedron* **1999**, *55*, 12657–12698.
- (2) Oyoung, C. L.; Pellet, R. J.; Casey, D. G.; Ugolini, J. R.; Sawicki, R. A. Skeletal Isomerization of 1-Butene on 10-Member Ring Zeolite Catalysts. *J. Catal.* **1995**, *151*, 467–469.
- (3) Seo, G.; Jeong, H. S.; Hong, S. B.; Uh, Y. S. Skeletal Isomerization of 1-Butene over Ferrierite and ZSM-5 Zeolites: Influence of Zeolite Acidity. *Catal. Lett.* **1996**, *36*, 249–253.
- (4) Méariaudeau, P.; Naccache, C. Skeletal Isomerization of n-Butenes Catalyzed by Medium-Pore Zeolites and Aluminosilicates. *Adv. Catal.* **1999**, *44*, 505–543.
- (5) Sato, T.; Dakka, J.; Sheldon, R. A. Titanium-Substituted Zeolite Beta(Ti-Al- $\beta$ )-Catalysed Epoxidation of Oct-1-ene with Tert-butyl Hydroperoxide (TBHP). *J. Chem. Soc., Chem. Commun.* **1994**, *16*, 1887–1888.
- (6) Semelsberger, T. A.; Ott, K. C.; Borup, R. L.; Greene, H. L. Role of acidity on the hydrolysis of dimethyl ether (DME) to methanol. *Appl. Catal., B* **2005**, *61*, 281–287.
- (7) Maihom, T.; Namuangruk, S.; Nanok, T.; Limtrakul, J. Theoretical Study on Structures and Reaction Mechanisms of Ethylene Oxide Hydration over H-ZSM-5: Ethylene Glycol Formation. *J. Phys. Chem. C* **2008**, *112*, 12914–12920.
- (8) Namuangruk, S.; Meeprasert, J.; Khemthong, P.; Faungnawakij, K. A Combined Experimental and Theoretical Study on the Hydrolysis of Dimethyl Ether over H-ZSM-5. *J. Phys. Chem. C* **2011**, *115*, 11649–11656.
- (9) Kondo, J. N.; Domen, K.; Wakabayashi, F. A Novel Route of Double-Bond Migration of an Olefin without Protonated Species on ZSM-5 Zeolite. *J. Phys. Chem. B* **1997**, *101*, 5477–5479.
- (10) Kondo, J. N.; Domen, K.; Wakabayashi, F. Double Bond Migration of 1-Butene Without Protonated Intermediate on D-ZSM-5. *Microporous Mesoporous Mater.* **1998**, *21*, 429–437.
- (11) Xu, T.; Munson, E. J.; Haw, J. F. Toward a Systematic Chemistry of Organic Reactions in Zeolites: In situ NMR Studies of Ketones. *J. Am. Chem. Soc.* **1994**, *116*, 1962–1972.
- (12) Biaglow, A. I.; Sepa, J.; Gorte, R. J.; White, D. A  $^{13}\text{C}$  NMR Study of the Condensation Chemistry of Acetone and Acetaldehyde Adsorbed at the Brønsted Acid Sites in H-ZSM-5. *J. Catal.* **1995**, *151*, 373–384.
- (13) Dumitriu, E.; Hulea, V.; Fechete, I.; Auroux, A.; Lacaze, J.-F.; Guimon, C. The Aldol Condensation of Lower Aldehydes over MFI Zeolites with Different Acidic Properties. *Microporous Mesoporous Mater.* **2001**, *43*, 341–359.
- (14) Solans-Monfort, X.; Bertran, J.; Branchadell, V.; Sodupe, M. Keto-Enol Isomerization of Acetaldehyde in HZSMS. A Theoretical Study Using the ONIOM2 Method. *J. Phys. Chem. B* **2002**, *106*, 10220–10226.
- (15) Shen, J. P.; Sun, L.; Song, C. Shape-Selective Synthesis of 4,4'-Dimethylbiphenyl. 1. Methylation of 4-Methylbiphenyl over Modified Zeolite Catalysts. *Catal. Lett.* **2000**, *65*, 147–151.
- (16) Guo, X.; Shen, J. P.; Sun, L.; Song, C.; Wang, X. Shape-Selective Methylation of 4-Methylbiphenyl to 4,4-Dimethylbiphenyl over Zeolite ZSM-5 Modified with Metal Oxides of MgO, CaO, SrO, BaO, and ZnO. *Catal. Lett.* **2003**, *87*, 25–29.
- (17) Maihom, T.; Boekfa, B.; Sirijaraensre, J.; Nanok, T.; Probst, M.; Limtrakul, J. Reaction Mechanisms of the Methylation of Ethene with Methanol and Dimethyl Ether over H-ZSM-5: An ONIOM Study. *J. Phys. Chem. C* **2009**, *113*, 6654–6662.
- (18) Nie, X.; Janik, M. J.; Guo, X.; Song, C. Shape-Selective Methylation of 2-Methylnaphthalene with Methanol over H-ZSM-5 Zeolite: A Computational Study. *J. Phys. Chem. C* **2012**, *116*, 4071–4082.
- (19) Hölderich, W.; Hesse, M.; Näumann, F. Zeolites: Catalysts for Organic Syntheses. *Angew. Chem., Int. Ed.* **1988**, *27*, 226–246.
- (20) Blasco, T.; Camblor, M. A.; Corma, A.; Perez-Pariente, J. P. The State of Ti in Titanooaluminosilicates Isomorphous with Zeolite  $\beta$ . *J. Am. Chem. Soc.* **1993**, *115*, 11806–11813.
- (21) Hutter, R.; Mallat, T.; Baiker, A. Titania Silica Mixed Oxides: II. Catalytic Behavior in Olefin Epoxidation. *J. Catal.* **1995**, *153*, 177–189.
- (22) Blasco, T.; Corma, A.; Navarro, M. T.; Pariente, J. P. Synthesis, Characterization, and Catalytic Activity of Ti-MCM-41 Structures. *J. Catal.* **1995**, *156*, 65–74.
- (23) Blasco, T.; Camblor, M. A.; Corma, A.; Esteve, P.; Guil, J. M.; Martinez, A.; Valencia, S. Direct Synthesis and Characterization of Hydrophobic Aluminum-Free Ti–Beta Zeolite. *J. Phys. Chem. B* **1998**, *102*, 75–88.
- (24) Li, K. T.; Chen, I. C. Epoxidation of Propylene on Ti/SiO<sub>2</sub> Catalysts Prepared by Chemical Vapor Deposition. *Ind. Eng. Chem. Res.* **2002**, *41*, 4028–4034.
- (25) Wang, S.; Liu, H. Selective Hydrogenolysis of Glycerol to Propylene Glycol on Cu–ZnO Catalysts. *Catal. Lett.* **2007**, *117*, 62–67.
- (26) Cortright, R. D.; Sanchez-Castillo, M.; Dumesic, J. A. Conversion of Biomass to 1,2-Propanediol by Selective Catalytic Hydrogenation of Lactic Acid over Silica-Supported Copper. *Appl. Catal., B* **2002**, *39*, 353–359.
- (27) Dasari, M. A.; Kiatimkul, P. P.; Sutterlin, W. R.; Suppes, G. J. Low-Pressure Hydrogenolysis of Glycerol to Propylene Glycol. *Appl. Catal., A* **2005**, *281*, 225–231.
- (28) Brönsted, J. N.; Kilpatrick, M.; Kilpatrick, M. Kinetic Studies on Ethylene Oxides. *J. Am. Chem. Soc.* **1929**, *51*, 428–461.
- (29) Long, F. A.; Pritchard, J. G. Hydrolysis of Substituted Ethylene Oxides in H<sub>2</sub>O<sup>18</sup> Solutions. *J. Am. Chem. Soc.* **1956**, *78*, 2663–2667.
- (30) Pritchard, J. G.; Long, F. A. Kinetics and Mechanism of the Acid-Catalyzed Hydrolysis of Substituted Ethylene Oxides. *J. Am. Chem. Soc.* **1956**, *78*, 2667–2670.
- (31) Parker, R. E.; Isaacs, N. S. Mechanisms of Epoxide Reactions. *Chem. Rev.* **1959**, *59*, 737–799.
- (32) Lundin, A.; Panas, I.; Ahlberg, E. A Mechanistic Investigation of Ethylene Oxide Hydrolysis to Ethanediol. *J. Phys. Chem. A* **2007**, *111*, 9087–9092.
- (33) Muniz Filho, R. C. D.; Sousa, S. A. A. D.; Pereira, F. D. S.; Ferreira, M. M. C. Theoretical Study of Acid-Catalyzed Hydrolysis of Epoxides. *J. Phys. Chem. A* **2010**, *114*, 5187–5194.
- (34) Li, Y.; Yue, B.; Yan, S.; Yang, W.; Xie, Z.; Chen, Q.; He, H. Preparation of Ethylene Glycol via Catalytic Hydration with Highly Efficient Supported Niobia Catalyst. *Catal. Lett.* **2004**, *95*, 163–166.
- (35) Ogawa, H.; Miyamoto, Y.; Fujigaki, T.; Chihara, T. Ring-Opening of 1,2-Epoxyalkane with Alcohols over H-ZSM-5 in Liquid Phase. *Catal. Lett.* **1996**, *40*, 253–255.
- (36) Solans-Monfort, X.; Sodupe, M.; Mó, O.; Yáñez, M.; Elguero, J. Hydrogen Bond vs Proton Transfer in HZSMS Zeolite. A Theoretical Study. *J. Phys. Chem. B* **2005**, *109*, 19301–19308.
- (37) Koktailo, G. T.; Lawton, S. L.; Olson, D. H. Structure of Synthetic Zeolite ZSM-5. *Nature* **1978**, *272*, 437–438.
- (38) Olson, D. H.; Koktailo, G. T.; Lawton, S. L.; Meier, W. M. Crystal Structure and Structure-Related Properties of ZSM-5. *J. Phys. Chem.* **1981**, *85*, 2238–2243.
- (39) van Koningsveld, H.; van Bekkum, H.; Jansen, J. C. On the Location and Disorder of the Tetrapropylammonium (TPA) Ion in Zeolite ZSM-5 with Improved Framework Accuracy. *Acta Crystallogr., Sect. B: Struct. Sci.* **1987**, *43*, 127–132.
- (40) Borini, S.; Philipsen, P.; Yakovlev, A.; McCormack, D.; Patchkovskii, S.; Heine, T. *ADF, DFTB 2012, SCM, Theoretical Chemistry*; Vrije Universiteit: Amsterdam, 2012.
- (41) Frenzel, J.; Oliveira, A. F.; Duarte, H. A.; Heine, T.; Seifert, G. Z. Structural and Electronic Properties of Bulk Gibbsite and Gibbsite Surfaces. *Z. Anorg. Allg. Chem.* **2005**, *631*, 1267–1271.
- (42) Guimaraes, L.; Enyashin, A. N.; Frenzel, J.; Heine, T.; Duarte, H. A.; Seifert, G. Imogolite Nanotubes: Stability, Electronic, and Mechanical Properties. *ACS Nano* **2007**, *1*, 362–368.
- (43) Luschnitz, R.; Oliveira, A. F.; Frenzel, J.; Joswig, J. O.; Seifert, G.; Duarte, H. A. Adsorption of Phosphonic and Ethylphosphonic Acid on Aluminum Oxide Surfaces. *Surf. Sci.* **2008**, *602*, 1347–1359.
- (44) Luschnitz, R.; Frenzel, J.; Milek, T.; Seifert, G. Adsorption of Phosphonic Acid at the TiO<sub>2</sub> Anatase (101) and Rutile (110) Surfaces. *J. Phys. Chem. C* **2009**, *113*, 5730–5740.

- (45) Baerends, E. J.; et al. ADF 2012.01, *Theoretical Chemistry*; SCM, Vrije Universiteit: Amsterdam, 2012.
- (46) Fonseca Guerra, C.; Snijders, J. G.; te Velde, G.; Baerends, E. J. Towards an Order-N DFT Method. *Theor. Chem. Acc.* **1998**, *99*, 391–403.
- (47) te Velde, G.; Bickelhaupt, F. M.; Baerends, E. J.; Fonseca Guerra, C.; van Gisbergen, S. J.; Snijders, J. G.; Ziegler, T. Chemistry with ADF. *J. Comput. Chem.* **2001**, *22*, 931–967.
- (48) Swart, M.; Bickelhaupt, F. M. QUILD: QUantum-regions Interconnected by Local Descriptions. *J. Comput. Chem.* **2008**, *29*, 724–734.
- (49) Swart, M.; Bickelhaupt, F. M. Optimization of Strong and Weak Coordinates. *Int. J. Quantum Chem.* **2006**, *106*, 2536–2544.
- (50) Becke, A. D. Density-Functional Exchange-Energy Approximation with Correct Asymptotic Behavior. *Phys. Rev. A* **1988**, *38*, 3098–3100.
- (51) Perdew, J. P. Density-Functional Approximation for the Correlation Energy of the Inhomogeneous Electron Gas. *Phys. Rev. B* **1986**, *33*, 8822–8824.
- (52) Grimme, S.; Antony, J.; Ehrlich, S.; Krieg, H. A Consistent and Accurate *Ab Initio* Parametrization of Density Functional Dispersion Correction (DFT-D) for the 94 Elements H-Pu. *J. Chem. Phys.* **2010**, *132*, 154104.
- (53) Snijders, J. G.; Baerends, E. J.; Vernooijns, P. Roothaan-Hartree-Fock-Slater Atomic Wave Functions. Single-Zeta, Double-Zeta, and Extended Slater-Type Basis Sets for  $^{87}\text{Fr}$ - $^{103}\text{Lr}$ . *At. Data Nucl. Data Tables* **1982**, *26*, 483–509.
- (54) Klamt, A.; Schüürmann, G. COSMO: A New Approach to Dielectric Screening in Solvents with Explicit Expressions for the Screening Energy and its Gradient. *J. Chem. Soc., Perkin Trans. 2* **1993**, 799–805.
- (55) Klamt, A. Conductor-like Screening Model for Real Solvents: A New Approach to the Quantitative Calculation of Solvation Phenomena. *J. Phys. Chem.* **1995**, *99*, 2224–2235.
- (56) Klamt, A.; Jones, V. Treatment of the Outlying Charge in Continuum Solvation Models. *J. Chem. Phys.* **1996**, *105*, 9972–9981.
- (57) Swart, M.; Rösler, E.; Bickelhaupt, F. M. Proton Affinities in Water of Main-group-Element Hydrides: Effects of Hydration and Methyl Substitution. *Eur. J. Inorg. Chem.* **2007**, 3646–3654.
- (58) Frenzel, J.; Oliveira, A. F.; Jardillier, N.; Heine, T.; Seifert, G. *Semi-relativistic, self-consistent charge Slater-Koster tables for density-functional based tight-binding (DFTB) for materials science simulations*; TU Dresden: Dresden, 2004–2009.
- (59) Du, X.; Wu, E. Porosity of Microporous Zeolites A, X and ZSM-5 Studied by Small Angle X-ray Scattering and Nitrogen Adsorption. *J. Phys. Chem. Solids* **2007**, *68*, 1692–1699.
- (60) Hudc, P.; Smiešková, A.; Žídek, Z.; Zúbek, M.; Schneider, P.; Kočírk, M.; Kozáková, J. Adsorption Properties of ZSM-5 Zeolites. *Collect. Czech. Chem. Commun.* **1998**, *63*, 141–154.
- (61) Treacy, M. M. J.; Foster, M. D. Packing Sticky Hard Spheres into Rigid Zeolite Frameworks. *Microporous Mesoporous Mater.* **2009**, *118*, 106–114.